Electronic Supplementary Information

Precious metal-free solar water splitting cell with bifunctional cobalt phosphide electrocatalyst and doubly promoted bismuth vanadate photoanode

Jin Hyun Kim[a†], Suenghoon Han[a], Yim Hyun Jo[b], Yunji Bak[c] and Jae Sung Lee[d*]

Supplementary Experimental

Calculation of surface/bulk charge separation efficiency

For quantitative assessment of charge separation efficiency, photocurrent comparison between water oxidation/hole scavengers (H_2O_2, SO_3^{2-}) was used.

Water oxidation: $2H_2O + 4h^+ \rightarrow 4H^+ + O_2$, E^o=1.23 V_{RHE}

Sulfite oxidation: $SO_3^{2-} + h^+ \rightarrow SO_3^-$, E^o=0.73 V_{RHE}

Light absorption by a photocatalyst generates absorbed photocurrent (J_{abs}) that undergoes two major losses of bulk and surface recombination. Hence the measured photocurrent during water oxidation (J^{H2O}) is expressed by;

$J^{H2O} = J_{abs} \times \eta_{bulk} \times \eta_{surf}$

where η denotes the charge separation yield in the bulk of semiconductor (η_{bulk}) or on the surface (η_{surf}). Since the surface charge separation yield of SO_3^{2-} is almost 100% ($\eta_{surf} = 1$), as discussed above, the photocurrent from its oxidation can be expressed as follows:

$J^{SO3} = J_{abs} \times \eta_{bulk}$

For calculation of J_{abs} value, below correlation between absorbance and radiation proposed by Choi's group [1].

$P_d = P_0 10^{-A}$

$P_{abs} = P_0(1-10^{-A})$

P_0 (unit : $mWcm^{-2}nm^{-1}$) is provided power by solar simulator (in this case, AM 1.5G), P_{abs} is power of light actually absorbed by photoanode and P_d is power of light not absorbed to photoanode but dissipated (reflection & penetration). A is absorbance of photoanode (in this case, $BiVO_4$) and LHE (light harvesting efficiency) is defined as $1-10^{-A}$. So light which is not absorbed at photoanode will be 10^{-A}. Integrated $P_{abs}(\lambda)$ ($mWcm^{-2}nm^{-1}$) along with wavelength λ gives total power (unit of $mWcm^{-2}$) which is power of light absorbed by photoanode (maximum power of photoanode). Below formula shows such relationship for photon absorption (J_{abs}).

$$J_{abs}(\frac{mA}{cm^2}) = \int_{\lambda_1}^{\lambda_2} \frac{\lambda}{1240} P_{abs}(\lambda) d\lambda \quad (\frac{mW}{cm^2})$$

J_{abs} is avg. 5.23 mA/cm^2 for 1% Mo:$BiVO_4$ films, while J_{max} = 7.5 mA/cm^2 for 100% of LHE till 2.4 eV (516nm) threshold is assumed. Bulk and surf separation efficiencies were calculated by:

$\eta_{bulk} = J^{SO3} / J_{abs}$

$\eta_{surf} = J^{H2O} / J^{SO3}$

Supplementary Figures

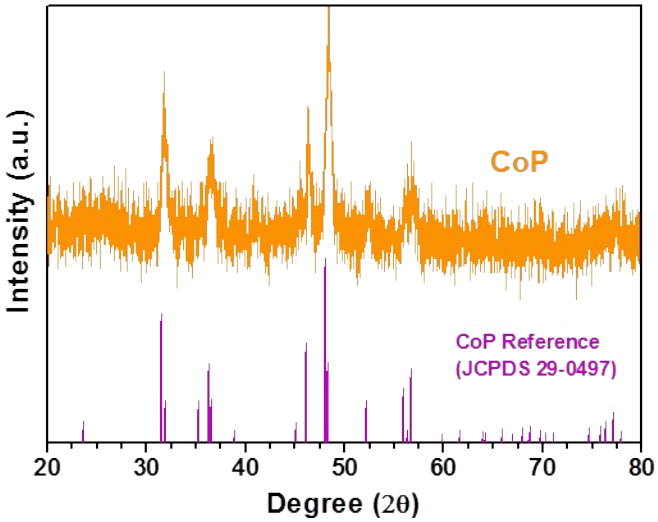

Figure S1. XRD results ofpurified CoP nanoparticles.

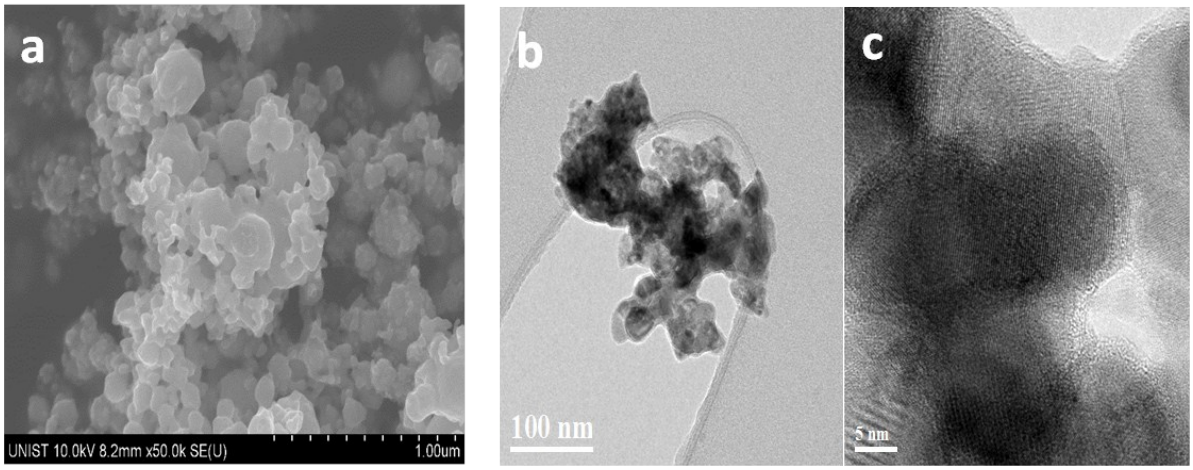

Figure S2. (a) SEM and (b,c) TEM images of CoP nanoparticles.

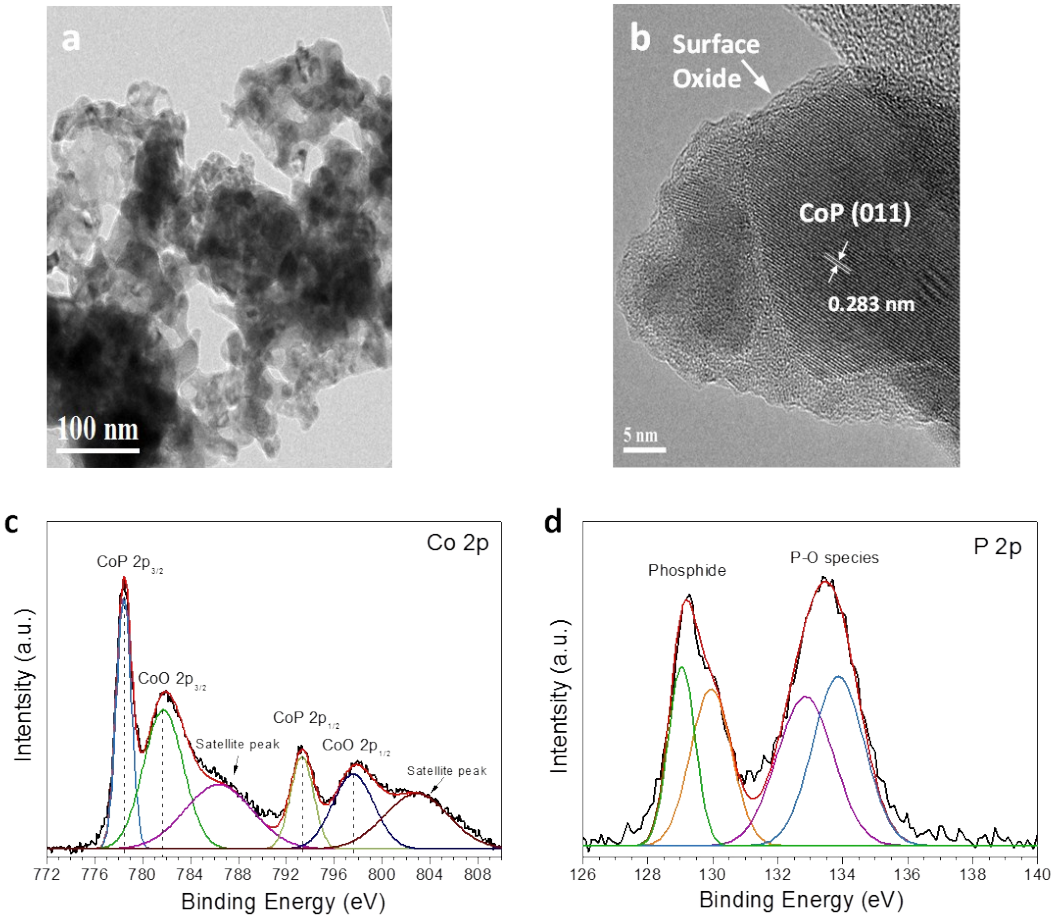

Figure S3. TEM images of (a) CoP nanoparticles, and (b) a magnified CoPnanoparticle. XPS spectra for (c) Co 2p and (d) P 2p of CoP nanoparticles.

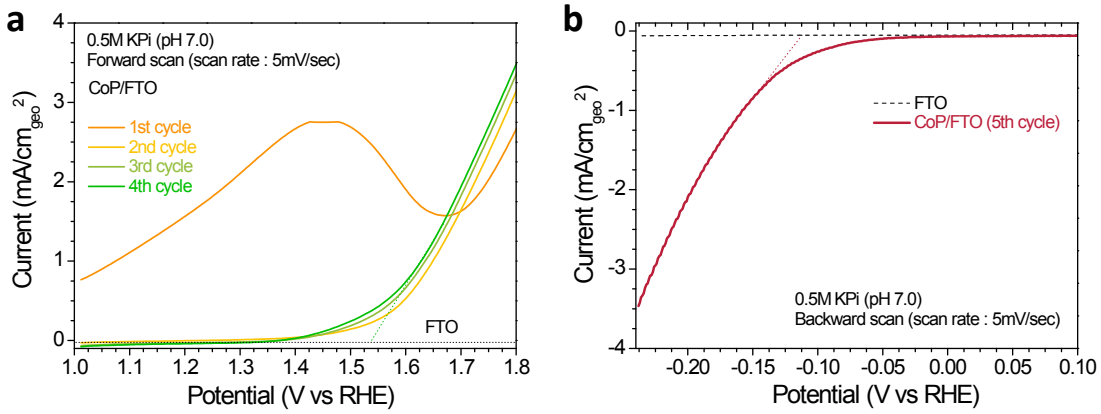

Figure S4. IV curves of CoP nanoparticlessuspension applied on FTO (a) anodic curve and (b) cathodic curve. Measurement conditions: electrolyte = 0.5 M Kpi (pH 7.0), CoP suspension loading = 2ul/0.7 cm^2 (FTO). Overall water splitting overpotential can be expressed as, $\eta_{overall}=\eta_{OER}$ (1.525 (onset potential for OER) – 1.23)– η_{HER} (0.0 – 0.1125 (onset potential for HER)) = 0.4075 V.

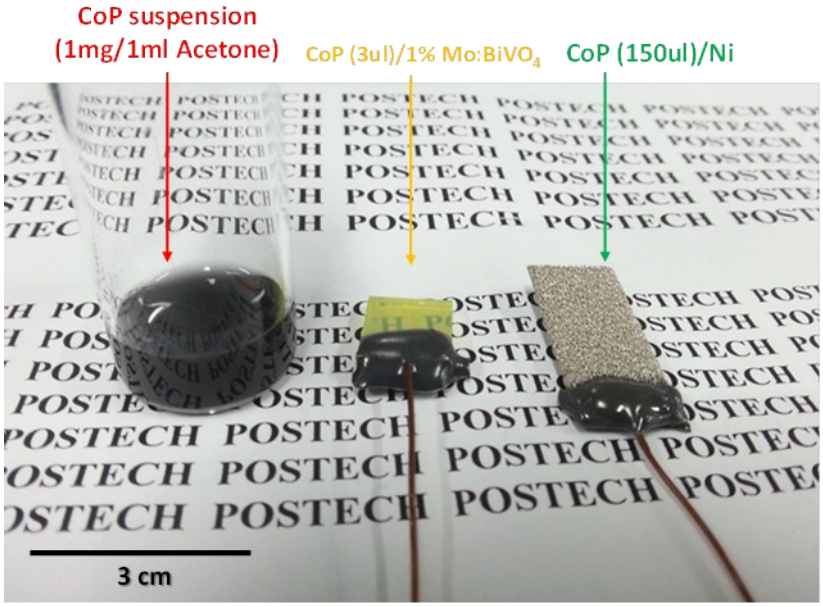

Figure S5. Pictures of CoP suspension, CoP/1% Mo:$BiVO_4$photoanode, and CoP/Ni foam cathode used for experiments. Small inset is CoP/1% Mo:$BiVO_4$ photoanode in action showing evolution of O_2 bubbles under simulated solar illumination (AM 1.5G) with an applied bias of 1.0 V_{RHE}.

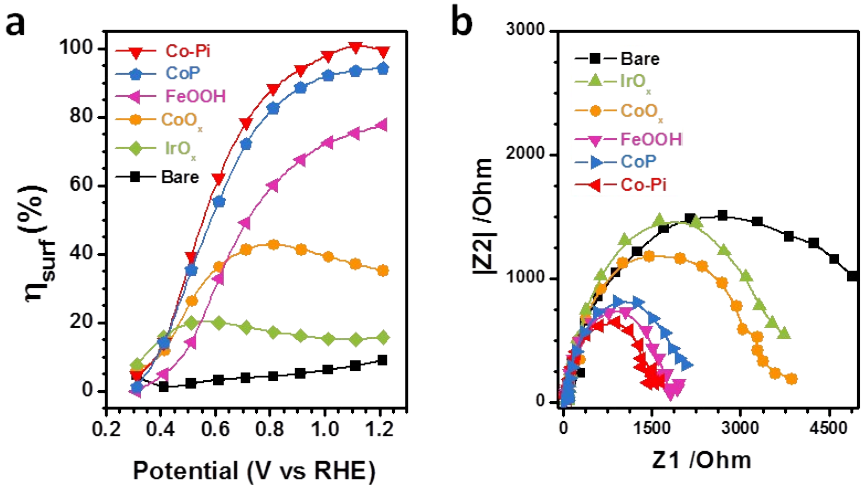

Figure S6. (a) Surface charge separation efficiency (η_{surf}) of photoanodes. (b) Nyquist plots of 1% Mo:$BiVO_4$ photoanode modified with various electrocatalysts with 1.23 V_{RHE} of applied potential. Measurement conditions: AM 1.5G (100 mW/cm^2), electrolyte = 0.5 M KPi (pH 7.0), cathode = Pt rod.

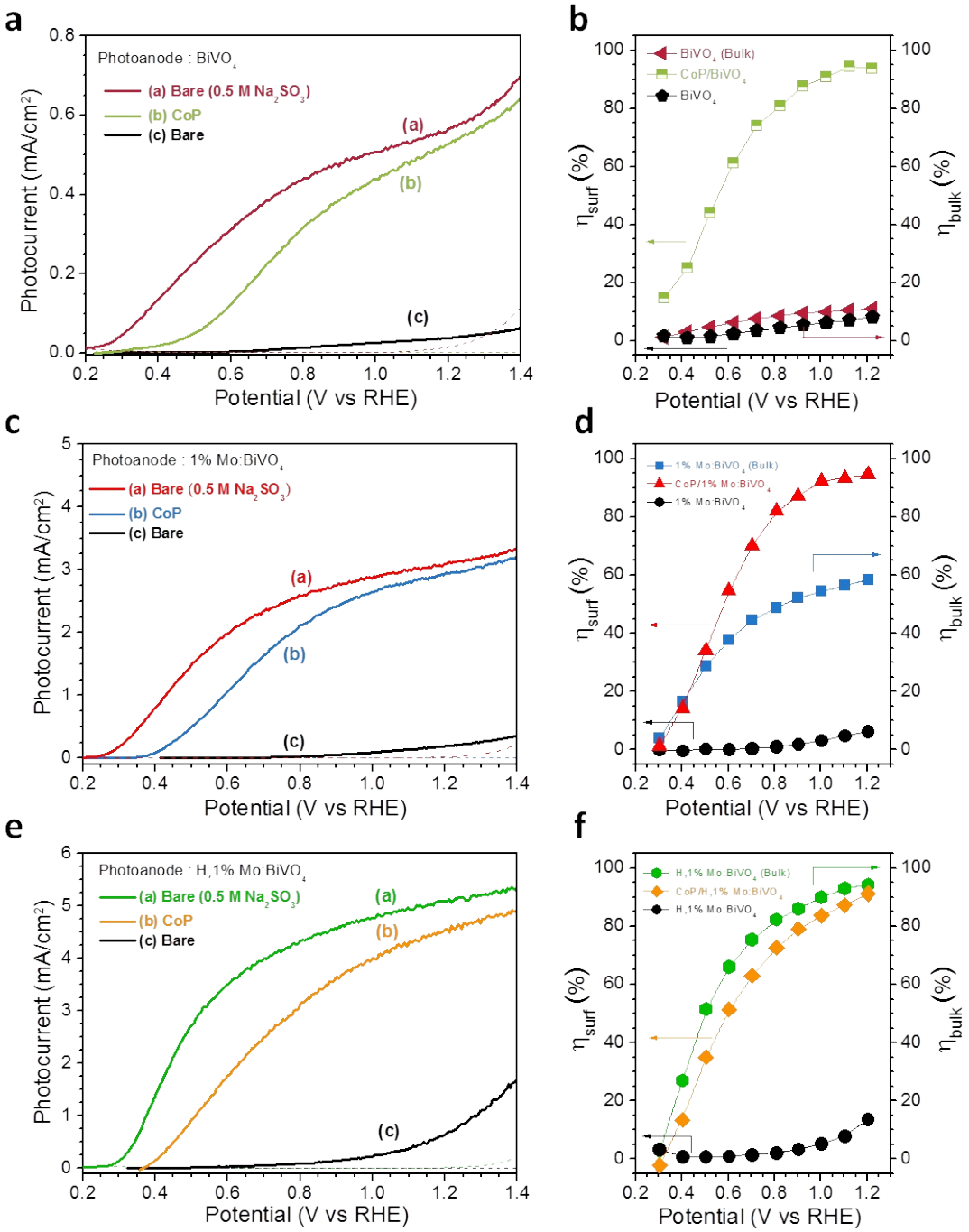

Figure S7. IV curves (a, c, e) and calculated charge separation efficiency (b, d, f) of bare $BiVO_4$, 1% Mo: $BiVO_4$ and H, 1% Mo: $BiVO_4$ modified by CoP loading. Measurement conditions: AM 1.5G illumination, electrolyte: 0.5 M KPi (pH 7.0), counter electrode: Pt rod. The η_{surf} and η_{bulk} values were calculated procedure was described in Supplementary Procedure of this SI with J_{abs} (absorption photocurrent) of $BiVO_4$ of 5.23 mA/cm^2. The $\eta_{surf}$is the ratio of currents obtained from photooxidation of water relative to that of the hole scavenger Na_2SO_3.

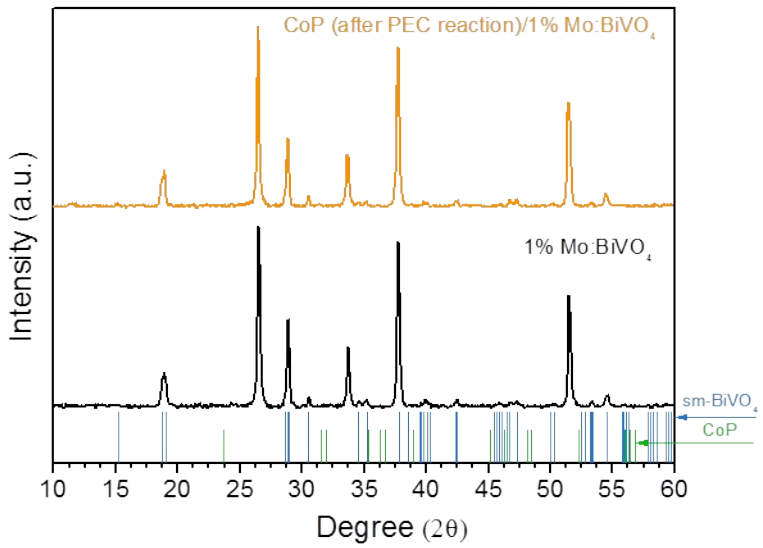

Figure S8. XRD spectra of 1% Mo:$BiVO_4$ and CoP loaded 1% Mo:$BiVO_4$ after PEC cell operation (~20 min). Below patterns are reference patterns of $BiVO_4$ (sheelite monoclinic, blue) and CoP (green).

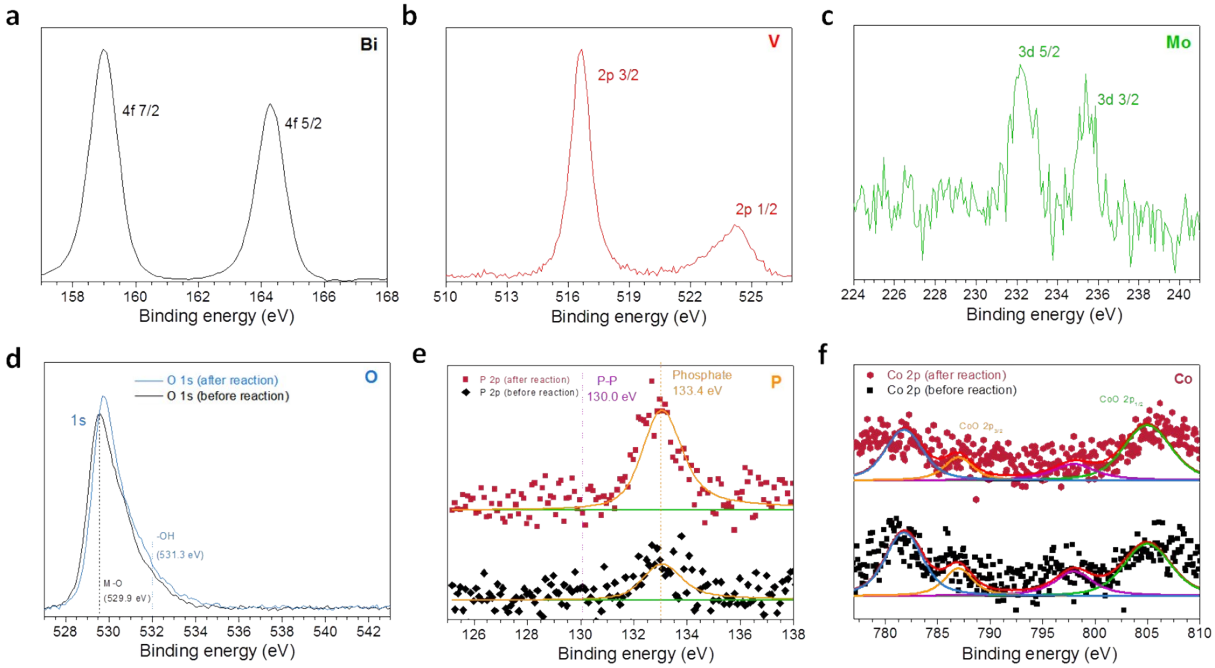

Figure S9. X-ray photoelectron spectra (XPS) of(a) Bi 4f, (b) V 2p and (c) Mo 3d of 1% Mo:$BiVO_4$(before PEC reaction) and (d) O 1s, (e) P 2p and (f) Co 2p of CoP/1% Mo:$BiVO_4$ before/after PEC water oxidation.

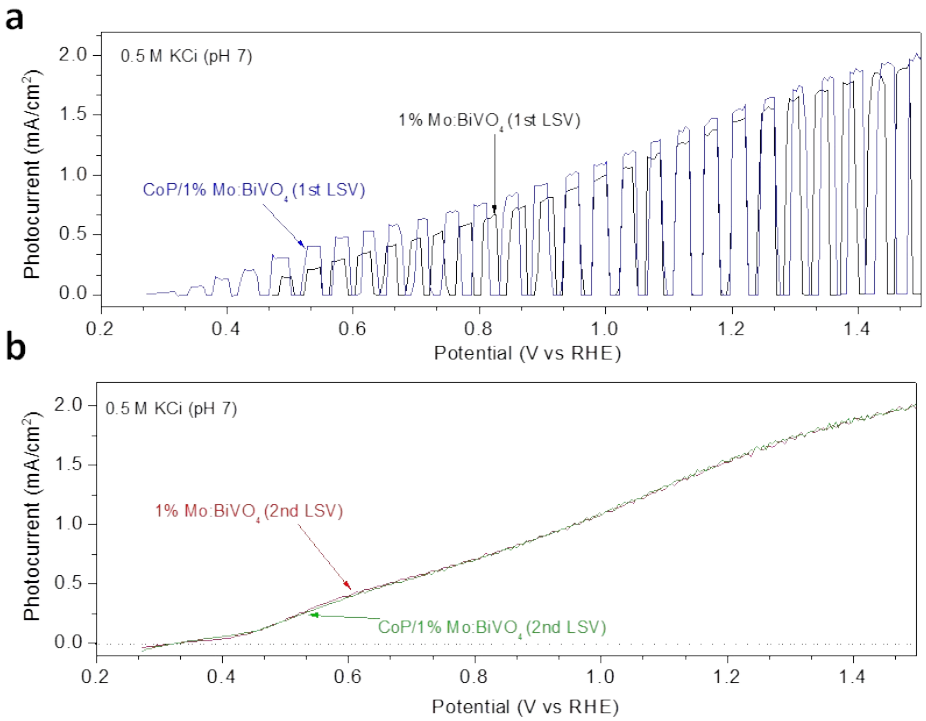

Figure S10. IV curve of 1% Mo:$BiVO_4$ with/without CoP loading with KCi electrolyte instead of KPi with similar pH (7.0). (a) 1st and (b) 2nd linear sweep. Measurement condition: AM 1.5G illumination, electrolyte: 0.5 M KCi (pH 7.0, CO_2 purged).

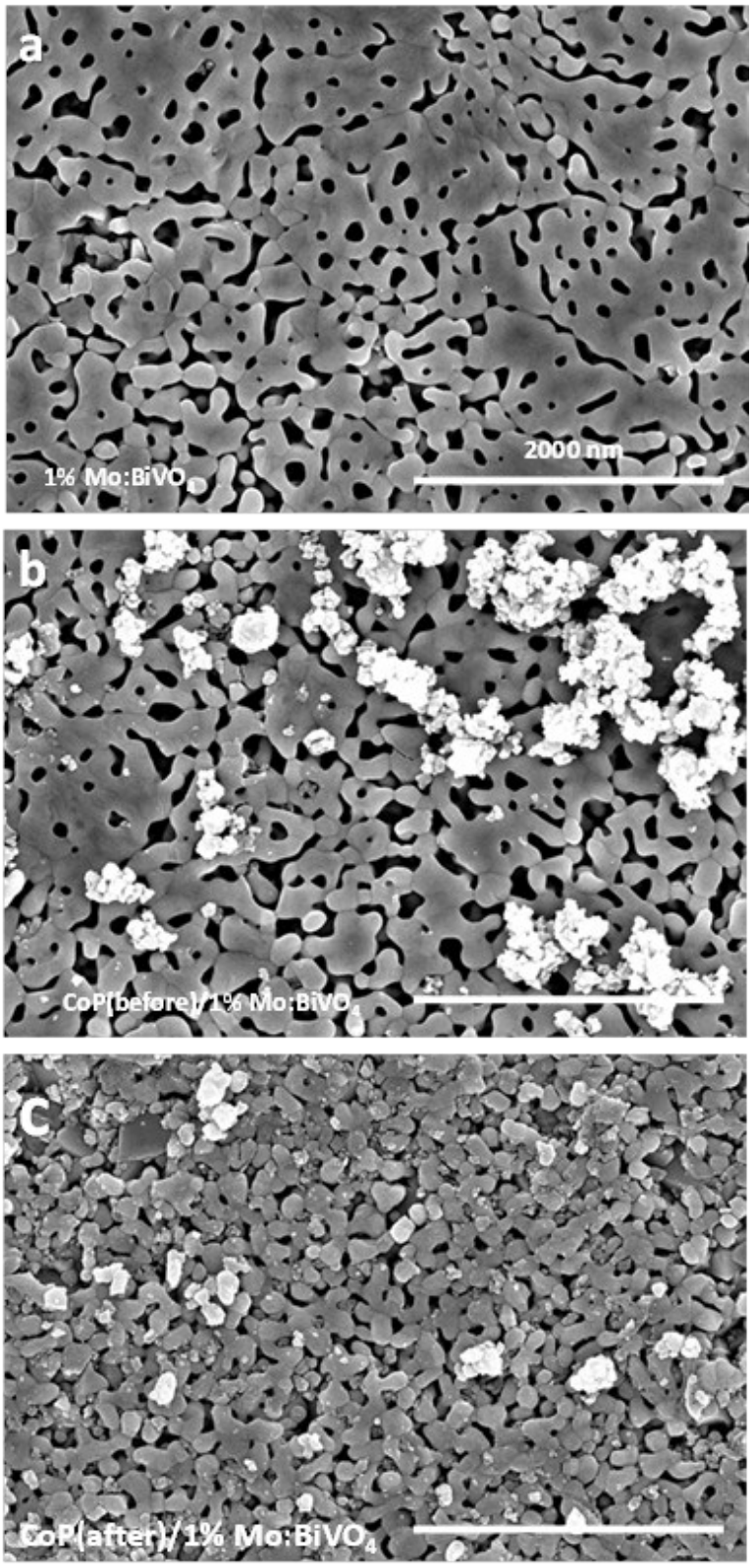

Figure S11. SEM images of (a) pristine surface of 1% Mo:$BiVO_4$, (b) CoP/1% Mo:$BiVO_4$ before PEC reaction and (c) CoP/1% Mo:$BiVO_4$ after PEC reaction. Large clusters of smaller CoP particles observed in (b) mostly disappear after PEC reaction in (c).

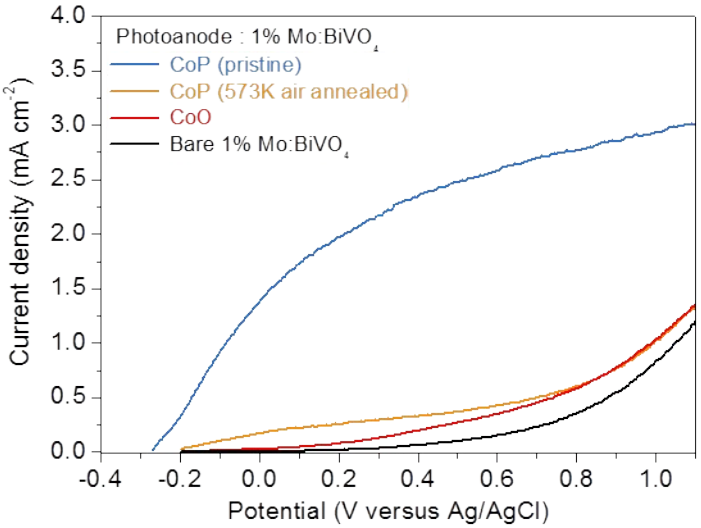

Figure S12. Optimization of the state of CoP loaded on 1% Mo:$BiVO_4$. Measurement conditions: AM 1.5G (100 mW/cm^2), electrolyte = 0.5 M KPi (pH 7.0), cathode = Pt rod.

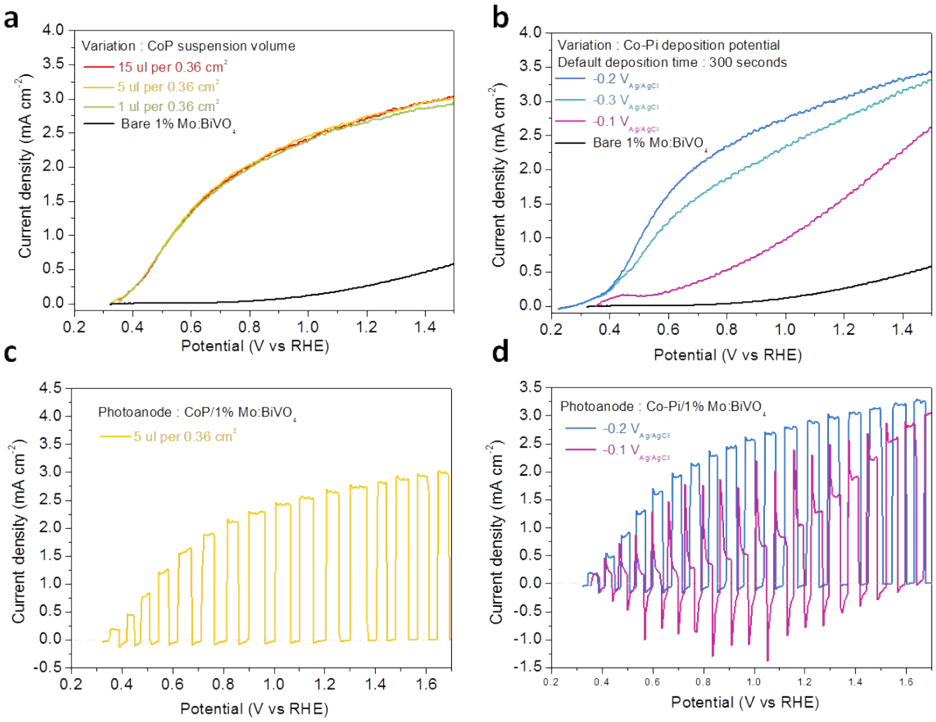

Figure S13. Optimization of CoP or Co-Pi loading amount on 1% Mo:$BiVO_4$. Measurement conditions: AM 1.5G (100 mW/cm^2), electrolyte = 0.5 M KPi (pH 7.0), cathode = Pt rod.

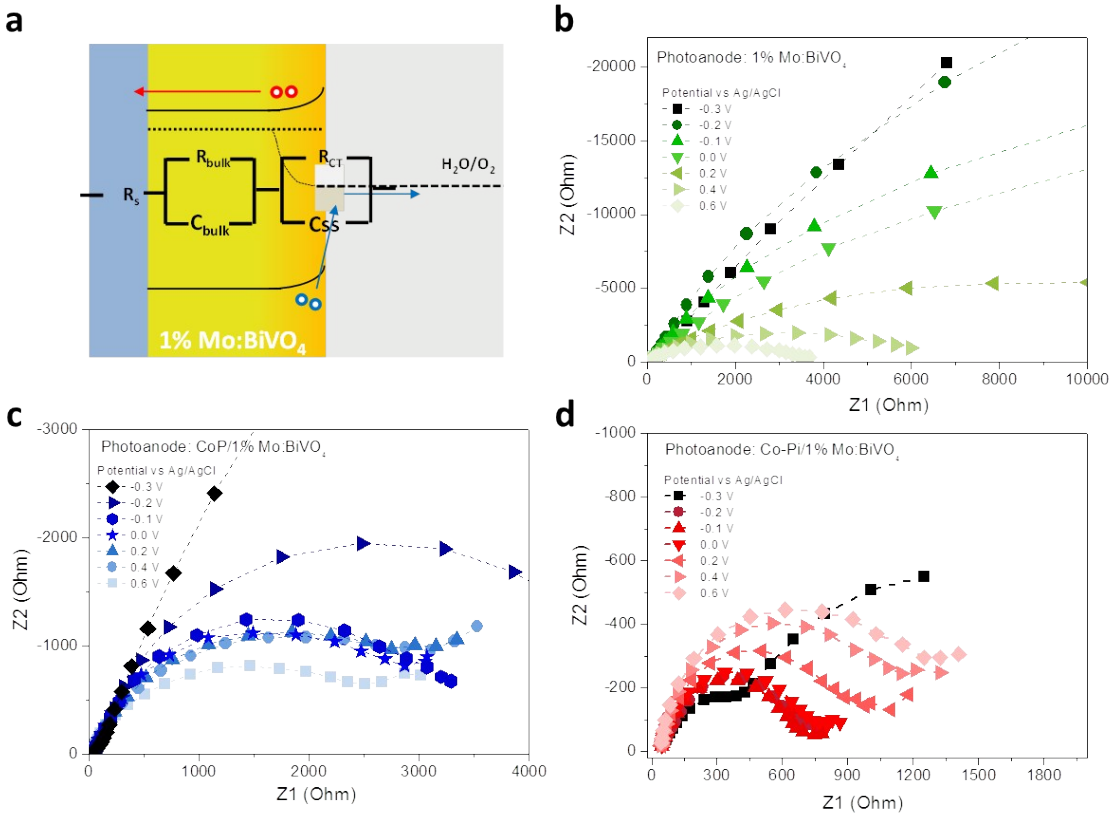

	1% Mo:$BiVO_4$	CoP/1% Mo:$BiVO_4$	Co-Pi/1% Mo:$BiVO_4$
Minimum R_{CT} (Ω) (potential)	3452	1635	675.5
	~1.2	0.48	0.48
Maximum C_{ss} (10^{4-} F/cm^2) (potential)	1.35	5.71	19.05
	0.90	~0.30	~0.30
J (mA/cm^2) at 1.23 V_{RHE}	0.12	2.86	3.1
Onset potential (V_{RHE})	0.587	0.307	0.252

Figure S14. (a) Equivalent (Randle) circuit model for curve fitting and (b-f) PEIS of 1% Mo:$BiVO_4$ and various surface modifications (bare, CoP and Co-Pi) with different bias range (-0.3 – 0.6 V vs. Ag/AgCl). Table includes parameters extracted from PEIS.

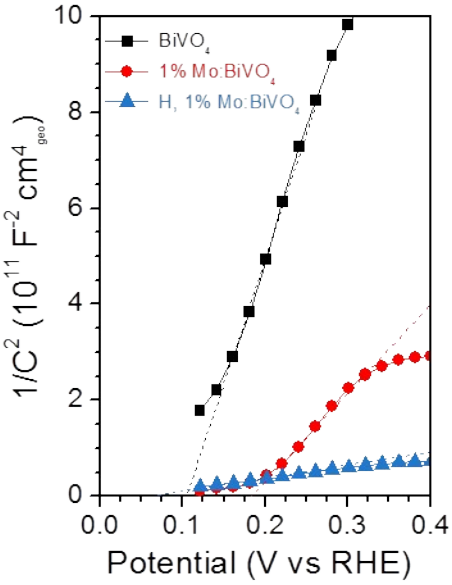

Figure S15. Mott-Schottky plots of $BiVO_4$-based photoanodes measured in 0.5 M KPi (pH 7.0) under dark, with a frequency of 1000 Hz and scan rate: 20mV/sec.

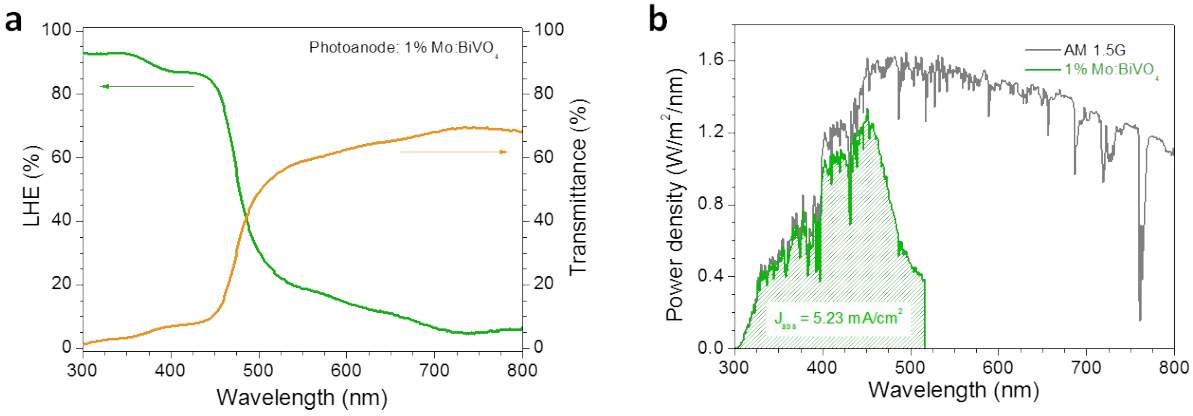

Figure S16. (a) Light harvesting efficiency (LHE), transmittance (T) of 1% $Mo:BiVO_4$ and (b) LHE corresponding to AM 1.5G spectrum. J_{abs} (absorption photocurrent) was calculated to be 5.23 mA/cm² with the procedure described in Supplementary Procedure of this ESI.

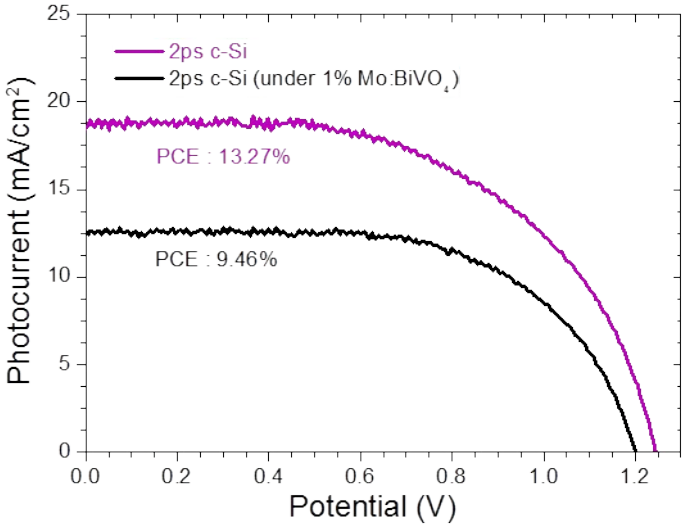

Figure S17. IV curves of (b) 2ps c-Si solar cell with/without 1% Mo:$BiVO_4$ filter.

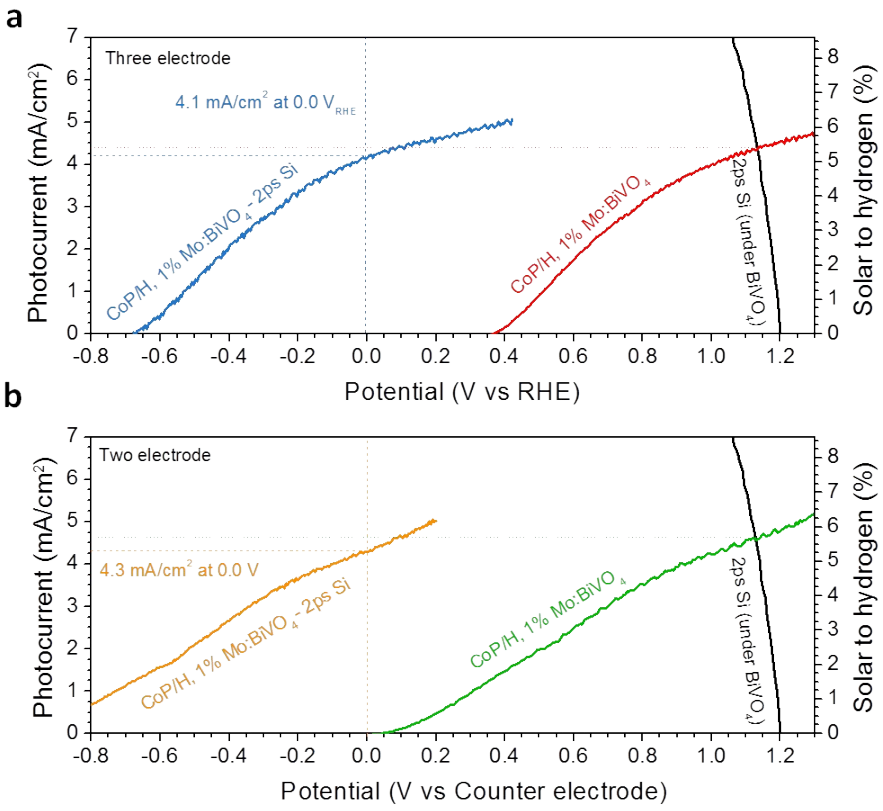

Figure S18. Tandem cell operating points determined by performance curves of the CoP/H, 1%Mo:$BiVO_4$photoanodes and solar cell (2ps c-Si) and actual operation of tandem cell with applied bias of 0.0 V_{RHE}. (a) Three electrode measurement. (b) Two electrode measurement. Measurement conditions: AM 1.5G illumination, electrolyte : 0.5 M KPi (pH 7.0).

Supplementary Tables

Table S1. Electrochemical hydrogen evolution reaction from water.

Catalysts	Onset potential [mV]	$\eta(10mA/cm^2)$ [mV]	Tafel Slope [mV dec^{-1}]	Electrolyte
CoP	61	145	62	1.0M H_2SO_4
CoP	71	205	97	1.0M KPi
CoP	78	170	151	1.0M NaOH
Pt/C	0	57	31	1.0M H_2SO_4
Pt/C	0	77	36	1.0M KPi
Pt/C	0	70	52	1.0M NaOH

Table S2. Recent reports on electrocatalyst/$BiVO_4$ based photoanode for solar water oxidation (2006-2017).

*Ref.	Photoanode (electrocatalyst/semiconductor)	**Electrolyte (pH)	***Method	****Feature	Ref
(1)	$Ag^+/BiVO_4$	0.1 M $Na2SO_4$ (pH ~7.0)	Dip in Ag+ solution	Cation exchange in $BiVO_4$ surface	8
(2)	$CoO_x/BiVO_4$	0.5 M $Na2SO_4$ (pH ~7.0)	Wet impregnation + annealing	(light source : 1000 W, > 420 nn)	9
(3)	RhO_x/Mo:$BiVO_4$	Sea water	Wet impregnation + annealing	~2.7 mA/cm^2 (1.23V_{RHE}), Sea water oxidation	10
(4)	Co-Pi/W:$BiVO_4$	0.1 M KPi (pH 8.0)	PED	~1.3 mA/cm^2 (1.23V_{RHE}) 440 mV cathodic onset potential shift Complete charge separation (η_{surf} = 100%)	5
(5)	Co-Pi/$BiVO_4$	0.1 M KPi (pH 7.0)	ED, PD, PED	Comparison of Co-Pi deposition method	7
(6)	CoO_x, IrO_x, MnO_x, RuO_x/$BiVO_4$	0.1 M KPi (pH 7.0)	Wet impregnation + annealing	Comparison with PEC and water oxidation	11
(7)	Pt/Mo, W:$BiVO_4$	0.1 M KPi + Na_2SO_4 (pH 7.0)	PD	~2.0 mA/cm^2 (1.23V_{RHE})	12
(8)	FeOOH/$BiVO_4$	0.1 M KPi (pH 7.0)	PED	~1.8 mA/cm^2 (1.23V_{RHE}) +6 h stable (η_{surf} = ~100%)	13
(9)	Co-Bi/$BiVO_4$	0.2 M KBi + Na2SO4 (pH 9.0)	ED	~2.0 mA/cm^2 (0.4 V_{SCE}) (light source : 300 W Xe, > 420 nm)	14
(10)	Ni-Bi/$BiVO_4$	0.1 M KBi (pH 9.2)	ED, PD	~1.2 mA/cm^2 (1.23V_{RHE})	15
(11)	Co-Pi/W:$BiVO_4$	0.1M KPi (pH 7.0)	PED	~3.6 mA/cm^2 (1.23V_{RHE}), Tandem cell with 2jn a-Si (STH = ~5%)	16
(12)	Co-Pi/$BiVO_4$/W:$BiVO_4$	0.1M KPi (pH 7.0)	PED	~4.0 mA/cm^2 (1.23V_{RHE}), Tandem cell with 2jn a-Si (STH = 5.2%)	17
(13)	$MnO_x/BiVO_4$	0.5 M K_2SO_4 (pH 6.8)	PD	Preferential deposition on specific (110) facet	18
(14)	$CoO_x/BiVO_4$	1 M NaOH(pH13.6)	ALD	~1.5 mA/cm^2 (1.23 V_{RHE}) Stable in pH 13.6	19
(15)	$PdO_x/BiVO_4$	0.1 M KPi (pH 7.0)	Wet impregnation + annealing	~1.1 mA/cm^2 (1.23V_{RHE}) Comparable with Co-Pi (η_{surf} = ~90%)	20
(16)	Ni/TiO_2/$BiVO_4$	1 M NaOH(pH13.6)	ALD (Ni)/ALD (TiO_2)	~1.2 mA/cm^2 (1.23V_{RHE}) Stable in pH 13.6	21
(17)	NiOOH/FeOOH /$BiVO_4$	0.5 M KPi (pH 7)	PED	~4.3 mA/cm^2 (1.23 V_{RHE}) Immense +48 h stable	22
(18)	$NiFeO_x/BiVO_4$	1 M NaOH	Metal organic decomposition	~0.6 mA/cm^2 (1.23V_{RHE})	23
(19)	Ru cat./$BiVO_4$	0.1 M KPi (pH 7)	Metal complex preparation + absorption	~1.2 mA/cm^2 (1.23V_{RHE}) Comparable with Co-Pi	24
(20)	Ni-Ci/W:$BiVO_4$	0.1 M KCi	PED	~2.0 mA/cm^2 (1.23 V_{RHE})	25

		(pH 7)		+24 h stable	
(21)	Co-Al LDH/$BiVO_4$	0.1 M KPi (pH 7)	Hydrothermal	~1.0 mA/cm^2 (1.23V_{RHE})	26
(22)	$NiO_x/CoO_x/BiVO_4$	0.1 M KPi (pH 7)	ALD/ALD	~3.5 mA/cm^2 (1.23V_{RHE})	27
(23)	Co-Ci/H, Mo:$BiVO_4$	0.1 M KCi (pH 7, 9)	PED	~4.8 mA/cm^2 (1.23V_{RHE}) +12 h stable Tandem cell with Perovskite so lar cell (STH = ~5%)	28
(24)	TiCo or TiNi/$BiVO_4$	0.1 M KBi 0.2M Na_2SO_4 (pH 9.2)	Single solution precursor drop + electrodeposi tion	~1.5 mA/cm^2 (1.23V_{RHE}) Bifunctional (OER, HER) Half-life photo stability of 5 hr Tandem cell with TiCo or TiNi/p-Si photocathode	29
(25)	NiOOH/FeOOH/N_2:$BiVO_4$	0.5 M Kpi(pH 7)	PED	~5.0 mA/cm^2 (1.23 V_{RHE}) +20 h stable	30
(26)	$Co^{2+}/ZnFe_2O_4/BiVO_4$	0.1M KOH (pH 12)	Ion absorption/Ther mal conversion	~2.5 mA/cm^2 (1.23V_{RHE}) Basic electrolyte stability	31
(27)	$NiLaCeCoO_x$ (mixed)/$BiVO_4$	0.1M NaOH + 0.5M Na_2SO_4 (pH 13)	Precursor drop casting/anneali ng	~3.3 mA/cm^2 (1.23V_{RHE}) Optimum composition found by combinatorial scanning Basic electrolyte stability	32
(28)	Ni doped $CoO_x/BiVO_4$	0.5M Na_2SO_4 (pH 7.0)	Spray deposition	~2.5 mA/cm^2 (1.23V_{RHE})	33
(29)	NiFe-Bi/Mo:$BiVO_4$/Ni/Sn	1.0M KBi (pH 9.0)	In-situ photoelectroch emical deposition (via equlibrium of dissovled Ni/Fe species)	~3.8 mA/cm^2 (1.23V_{RHE}) +1100 h stability	34
(30)	Co-La double hydroxide/$BiVO_4$	0.5 M KPi (pH 7.0)	In-situ photoelectroch emical deposition	~2.1 mA/cm^2 (1.23V_{RHE}) +80% charge separation	35
This work	**CoP/H, 1% Mo:$BiVO_4$**	**0.5 M KPi** **(pH 7.0)**	**Particle drop + In-situ transitio n (via OER)**	~4.7 mA/cm^2 (1.23V_{RHE}) +4 h stable Tandem cell with c-Si PV (STH= ~5.3%)	

*Reports are arranged in year, but not in actual publication date.
**KPi : potassium biphosphate, KCi : potassium bicarbonate, KBi : Potassium borate
***PD : photodeposition, ED : electrodeposition, PED : photoelectrodeposition
****light source of all results are AM 1.5G, 100mW/cm^2 (1 sun) unless it is individually denoted.
η_{surf} = surface charge separation efficiency. (photocurrent ratio between oxidations of a sacrificial reagent and wate r).
Material is denoted as stable if constant potential operation was demonstrated without serious efficiency drop (<25%).

Supplementary references

1. H. W. Jeong, T. H. Jeon, J. S. Jang, W. Choi and H. Park, *J. Phys. Chem. C*, **2013**, 117, 9104-9112.
2. M. W. Kanan and D. G. Nocera, *Science*, **2008**, 321, 1072-1075.
3. M. W. Kanan, Y. Surendranath and D. G. Nocera, *Chem. Soc. Rev.*, **2009**, 38, 109-114.
4. G. M. Carroll, D. K. Zhong and D. R. Gamelin, *Energy Environ. Sci.*, **2015**.
5. D. K. Zhong, S. Choi and D. R. Gamelin, *J. Am. Chem. Soc.*, **2011**, 133, 18370-18377.
6. D. K. Zhong and D. R. Gamelin, *J. Am. Chem. Soc.*, **2010**, 132, 4202-4207.
7. T. H. Jeon, W. Choi and H. Park, *Phys. Chem. Chem. Phys.*, **2011**, 13, 21392-21401.
8. K. Sayama, A. Nomura, T. Arai, T. Sugita, R. Abe, M. Yanagida, T. Oi, Y. Iwasaki, Y. Abe and H. Sugihara, *J. Phys. Chem. B*, **2006**, 110, 11352-11360.
9. Long, Cai and H. Kisch, *J. Phys. Chem. C*, **2007**, 112, 548-554.
10. W. Luo, Z. Yang, Z. Li, J. Zhang, J. Liu, Z. Zhao, Z. Wang, S. Yan, T. Yu and Z. Zou, *Energy Environ. Sci.*, **2011**, 4, 4046-4051.
11. D. Wang, R. Li, J. Zhu, J. Shi, J. Han, X. Zong and C. Li, *J. Phys. Chem. C*, **2012**, 116, 5082-5089.
12. S. P. Berglund, A. J. E. Rettie, S. Hoang and C. B. Mullins, *Phys. Chem. Chem. Phys.*, **2012**, 14, 7065-7075.
13. K. J. McDonald and K.-S. Choi, *Chem. Mater.*, **2011**, 23, 4863-4869.
14. C. Ding, J. Shi, D. Wang, Z. Wang, N. Wang, G. Liu, F. Xiong and C. Li, *Phys. Chem. Chem. Phys.*, **2013**, 15, 4589-4595.
15. S. K. Choi, W. Choi and H. Park, *Phys. Chem. Chem. Phys.*, **2013**, 15, 6499-6507.
16. F. F. Abdi, L. Han, A. H. M. Smets, M. Zeman, B. Dam and R. van de Krol, *Nat. Commun.*, **2013**, 4, 2195.
17. L. Han, F. F. Abdi, R. van de Krol, R. Liu, Z. Huang, H.-J. Lewerenz, B. Dam, M. Zeman and A. H. M. Smets, *ChemSusChem.*, **2014**, 7, 2832-2838.
18. R. Li, F. Zhang, D. Wang, J. Yang, M. Li, J. Zhu, X. Zhou, H. Han and C. Li, *Nat. Commun.*, **2013**, 4, 1432.
19. M. F. Lichterman, M. R. Shaner, S. G. Handler, B. S. Brunschwig, H. B. Gray, N. S. Lewis and J. M. Spurgeon, *J. Phys. Chem. Lett.*, **2013**, 4, 4188-4191.
20. J. H. Kim, J. W. Jang, H. J. Kang, G. Magesh, J. Y. Kim, J. H. Kim, J. Lee and J. S. Lee, *Journal of Catalysis*, **2014**, 317, 126-134.
21. M. T. McDowell, M. F. Lichterman, J. M. Spurgeon, S. Hu, I. D. Sharp, B. S. Brunschwig and N. S. Lewis, *J. Phys. Chem. C*, **2014**, 118, 19618-19624.
22. T. W. Kim and K.-S. Choi, *Science*, **2014**, 343, 990-994.
23. J. H. Kim, H. J. Kang, M. Ganesan and J. S. Lee, *Rapid Communication in Photoscience*, **2014**, 3, 35-37.
24. M. de Respinis, K. S. Joya, H. J. M. De Groot, F. D'Souza, W. A. Smith, R. van de Krol and B. Dam, *J. Phys. Chem. C*, **2015**, 119, 7275-7281.
25. S. K. Pilli, K. Summers and D. Chidambaram, *RSC Adv.*, **2015**, 5, 47080-47089.
26. W. He, R. Wang, L. Zhang, J. Zhu, X. Xiang and F. Li, *J. Mater. Chem. A*, **2015**, 3, 17977-17982.
27. M. Zhong, T. Hisatomi, Y. Kuang, J. Zhao, M. Liu, A. Iwase, Q. Jia, H. Nishiyama, T. Minegishi, M. Nakabayashi, N. Shibata, R. Niishiro, C. Katayama, H. Shibano, M. Katayama, A. Kudo, T. Yamada and K. Domen, *J. Am. Chem. Soc.*, **2015**, 137, 5053-5060.
28. J. H. Kim, Y. Jo, J. H. Kim, J. W. Jang, H. J. Kang, Y. H. Lee, D. S. Kim, Y. Jun and J. S. Lee, *ACS Nano*, **2015**, 9, 11820-11829.

29. Y.-H. Lai, D. W. Palm and E. Reisner, *Adv. Energy Mater.*, **2015**, 5, 1501668-n/a.
30. T. W. Kim, Y. Ping, G. A. Galli and K.-S. Choi, *Nat. Commun.*, **2015**, 6, 8769.
31. T. W. Kim and K.-S. Choi, *J. Phys. Chem. Lett.*, **2016**, 7, 447-451.
32. D. Guevarra, A. Shinde, S. K. Suram, I. D. Sharp, F. M. Toma, J. A. Haber and J. M. Gregoire, *Energy Environ. Sci.*, **2016**, 9, 565-580.
33. Y. Liu, Y. Guo, L. T. Schelhas, M. Li and J. W. Ager, *J. Phys. Chem. C*, **2016**, 120, 23449-23457.
34. Y. Kuang, Q. Jia, G. Ma, T. Hisatomi, T. Minegishi, H. Nishiyama, M. Nakabayashi, N. Shibata, T. Yamada, A. Kudo and K. Domen, *Nature Energy*, **2016**, 2, 16191.
35. M. Chhetri, S. Dey and C. N. R. Rao, *ACS Energy Letters*, **2017**, 2, 1062-1069.